ELSEVIER

Electronic structure and valence state of CeAl$_2$ from X-ray absorption and emission spectroscopy

C.L. Dong [a, b], A. Augustsson [a, c], C.L. Chen [b], C.L. Chang [b], Y.Y. Chen [d], J.-H. Guo [a, *]

[a] Advanced Light Source, Lawrence Berkeley National Laboratory, Berkeley, CA 94720, USA
[b] Department of Physics, Tamkang University, Tamsui 251, Taiwan, ROC
[c] Department of Physics, Uppsala University, Box 530, SE-75121 Uppsala, Sweden
[d] Institute of Physics, Academia Sinica, Taipei, Taiwan, ROC

Available online 19 February 2005

Abstract

Soft X-ray absorption spectroscopy (XAS) and resonant inelastic X-ray scattering (RIXS) have been performed on CeAl$_2$ bulk and nanoparticles of 8 nm to study the quantum size effect of this heavy-fermion compound. XAS and RIXS spectra recorded at selected photon energies, reflect the local unoccupied and occupied electronic states. These spectral shape changes are attributed to surface effects originated from the reducing particle size, which gives rise to different hybridization between the 4f orbitals and conduction band. The Ce in nanoparticles exhibits mixed valencies with a small portion of tetravalent Ce in contrast to the mostly trivalent Ce observed in the bulk CeAl$_2$. RIXS spectra show a strong dependence on the excitation energies. The experimental results suggest the different f-electron configurations for bulk and nanoparticle CeAl$_2$.
© 2005 Elsevier B.V. All rights reserved.

Keywords: X-ray absorption; X-ray emission

1. Introduction

The electronics industry is in need of the materials with ultrasmall sizes to be used in novel devices for technological applications [1]. Nanomaterials are materials in the intermediated dimensions between the atom and the solid, exhibiting electronic, magnetic and structural properties that are different from their bulk forms. The electronic structure is of important to understand the properties of these nanomaterials [2]. In a recent study [3] of heavy-fermion compound CeAl$_2$, the measurement of specific heat for 8 nm nanoparticles demonstrated that cerium atoms on the nanoparticle surface are nonmagnetic. Additionally, the antiferromagnetic transition ($T_N = 3.8$ K) observed in bulk CeAl$_2$ was not shown in the nanoparticles. The loss of magnetism was attributed to changes of the electronic structure induced by the reduced particle size.

In rare earth compounds, the information on f-electron occupancy is the key to understand the different physical phenomena. In correlated f-state system, the strong hybridization between 4f electron and the conduction electrons give rise to unusual physical properties, such as Kondo effect, valence fluctuation, and magnetic behavior. Since the f states can have both band-like and localized character, varying the strength of hybridization. In order to explore the effect of particle size on the electronic structures, we have performed X-ray absorption (XAS) and resonant inelastic X-ray scattering (RIXS) studies on CeAl$_2$ nanoparticles and bulk material.

2. Experimental details

CeAl$_2$ bulk was first prepared by arc melting the high-purity constituent elements Ce (99.9%) and Al (99.9999%) in an argon atmosphere (99.999%). The structure and phase purity were examined by powder X-ray diffraction and exhibits cubic Laves structure with a lattice constant $a_0 = 8.06$ Å

* Corresponding author. Tel.: +1 510 495 2230; fax: +1 510 486 7588.
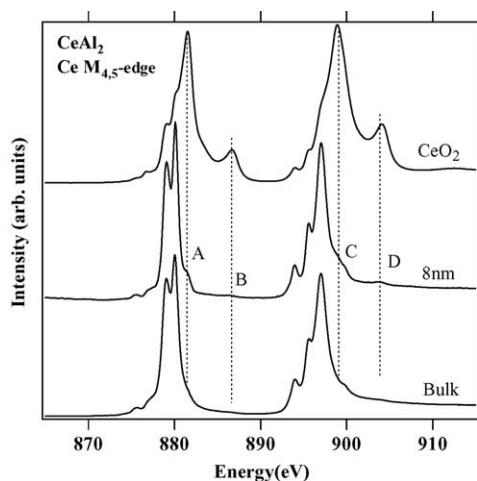 *E-mail address:* jguo@lbl.gov (J.-H. Guo).

Fig. 1. Ce $M_{4,5}$ absorption spectra of the $CeAl_2$ and CeO_2. Bulk $CeAl_2$ exhibits mostly $3d^9 4f^2$ final state with two main structures at around 880 and 897 eV. The features A–D in nanoparticles related to $3d^9 4f^1$ final states are indicated.

which is consistent with that of previous report [4]. Nanoparticles of $CeAl_2$ were then fabricated on a liquid-nitrogen cold trap by flash evaporation of bulk $CeAl_2$ in an atmosphere of 0.1 Torr of He gas. Details of the sample preparation procedure are described elsewhere [5]. The X-ray diffraction results of $CeAl_2$ nanoparticles show the pure single phase of $CeAl_2$ with no trace of CeO_2. The Ce $M_{4,5}$ absorption spectra were recorded at beamline HSGM in NSRRC, Taiwan. The Ce 4d absorption and RIXS spectra were measured on beamline 7.0.1 at ALS, LBNL. The RIXS spectra were normalized to the maximum of elastic feature.

3. Results and discussions

The XAS spectra at the Ce $M_{4,5}$-edge are shown in Fig. 1 along with the reference sample: CeO_2. In this case, a Ce 3d electron is excited to the 4f state or the valence band (5d6s) at the energy of Ce $M_{4,5}$-edge, that is, $3d^{10} 4f^m$ $VB^m \rightarrow 3d^9 4f^{m+1} VB^m$ or $3d^{10} 4f^m VB^m \rightarrow 3d^9 4f^m VB^{m+1}$. The former transition is the electron excited from 3d to 4f level. The later process is the excitation in which an electron goes into valence states due to the hybridization between 4f level and valence state as it was established in early report [6]. These two processes are of important for describing the XPS spectra. However, the later transition is too weak to be observed in XAS spectra. The spectrum of bulk $CeAl_2$ exhibits two main structures at around 880 and 897 eV due to the spin orbital splitting of $3d_{3/2}$ and $3d_{5/2}$ multiple structures of the $3d^9 4f^2$ final state. The line shape is quite similar to that of γ-Ce and very much different to that of CeO_2 (top curve), which implies the valence in bulk $CeAl_2$ is mainly +3. The spectrum of nanoparticles $CeAl_2$ shows enhanced features A and C and additional features B and D. The absorption features A–D coincide with the energy positions of the main features of CeO_2

and consequently can be assigned to the $3d^9 4f^1$ final states. This indicates that the $CeAl_2$ nanoparticles exhibits the mixture of $4f^1 (5d6s)^3$ and $4f^0 (5d6s)^4$ configurations in ground state, which is in consistent with the observation from Ce L_3-edge. The strength of hybridization of the f-state and conduction state can be estimated from the spectral profile [7]. The growth of features A–D in nanoparticles indicates stronger interaction of the 4f level and conduction band with respect to the bulk $CeAl_2$.

The Ce 4d absorption promotes a 4d electron to a 4f state. The XAS spectra, displayed in Fig. 2, represent the excitation of $4d^{10} 4f^m$ ground state to $4d^9 4f^{m+1}$ final state. The shape of 4d absorption spectra is very sensitive to the occupancy of the 4f state. The spectra consist of two regions: a group of fine structures from 102 to 114 eV, and a strong broad band in the energy region of 115–130 eV. The fine structures are interpreted as transitions to multiplet splitting of $4d^9 4f^{m+1}$ configuration as a result of the exchange and Coulomb interactions between 4d hole and 4f electrons due to the radial overlap of the 4d and 4f wave functions [8–10]. The broad band absorption has been observed in many Ce compounds [11]. This giant absorption resonance arises from a rapid decay of $4d^9 4f^{m+1}$ state into a continuum state. The XAS spectrum of bulk $CeAl_2$ in Fig. 2(a) exhibits one broad band A_1, which is similar to pure Ce and indicates the Ce in bulk $CeAl_2$ is trivalent ($4f^1$). However, the XAS results of Ce nanoparticles presented in Fig. 2(b) shows: in addition to feature A_1, another new broad feature A_2 is observed around 124 eV that is a characteristic of the tetravalent Ce. The energy position of feature A_1 and A_2 correspond to the Ce^{3+} and Ce^{4+} resonances observed in the resonant photoemission spectra [12]. This implies that a mixture of Ce^{3+} and Ce^{4+} exists in $CeAl_2$ nanoparticles.
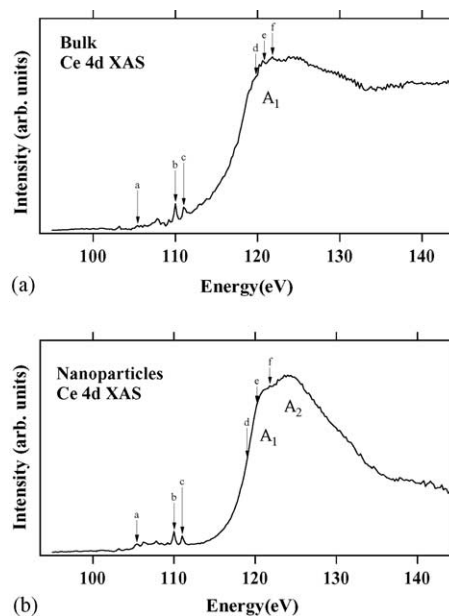

Fig. 2. Ce 4d-edge XAS spectra of bulk (a) and nanoparticle (b) $CeAl_2$.

RIXS has been found to be very useful to elucidate inner-shell excitation (f–f excitation) and charge transfer in rare earth systems [13,14]. The 4d RIXS spectra of bulk and nanoparticles $CeAl_2$ for various excitation energies are displayed in the energy-loss scales in Fig. 3. In order to obtain the energy-loss spectra, the energy of the emitted photons for each spectrum is subtracted from the incoming photon energies (excitation energy). The excitation energies were chosen as denoted by the letters d–f in the XAS spectrum. Strong spectral variations upon different excitation energies are observed. The spectra can be distinguished to three contributions, e.g., the elastic scattering radiation, of inelastic scattering and normal fluorescence emission.

The elastic scattering radiation (feature A) at energy-loss 0 eV is equal to incoming photon energy. The lowest energy excited feature B at about 4 eV, is resonantly enhanced when the energy is tuned to the XAS threshold energy. This feature is related to $4f^0$ character and can be an indicator of the hybridization strength between 4f level and conduction band [15]. All the energy-loss features of nanoparticles $CeAl_2$ (see in Fig. 3(b)) are more enhanced than that in the bulk $CeAl_2$ (Fig. 3(a)), which implies stronger hybridization resulting from the mixtures of $4f^0$, $4f^1$, and $4f^2$ states. The energy-loss features C at around 9 eV are mostly due to the $4f^2$ final states as a result of $f^1 \rightarrow f^2$ charge transfer excitation [16,17]. It is noticed that the RIXS features are more pronounced in nanoparticles sample (Fig. 3(b)) than in the bulk (Fig. 3(a)). However, in nanoparticles $CeAl_2$, apart from the $f^1 \rightarrow f^2$ charge transfer excitation, there may be a charge transfer from Al 3p valence bands to 4f levels through the

intermediate state $4d^9 5p^6 4f^1$ [16,18]. This charge transfer has been also observed in XAS studies for different thickness thin films of $CeAl_2$ [18]. Several weak fine structures D indicated by lines shift to higher energy-loss side as the excitation energies increase. These structures are assigned to the normal fluorescence emission due to $4f \rightarrow 4d$ transition, which reflects the 4f band information. The inelastic feature E represents the $5p \rightarrow 4f$ transitions in which a 5p electron is promoted to the 4f shell. It starts with the $4d^{10} 5p^6 4f^m$ initial state to the $4d^9 5p^6 4f^{m+1}$ intermediate state and then radiative decay to the $4d^{10} 5p^5 4f^{m+1}$ final state. Similar results are also observed in other lanthanides [19,20].

4. Conclusion

The size dependent valence change in nanoparticles $CeAl_2$ is observed in XAS spectra. The Ce in nanoparticles exhibits a mixed valency with a small portion of tetravalent Ce in contrast to the mostly trivalent Ce in bulk $CeAl_2$. We observed strong changes on the spectral shape of RIXS spectra upon the excitation energies. The spectral features at around 20–25 eV below the elastic peak correspond to the transitions between the $4d^{10} 5p^6 4f^m$ initial state and $4d^{10} 5p^5 4f^{m+1}$ final state and consequently assigned to Ce core-core transition (5p–4f emission). The energy-loss feature at 9 eV is contributed to the charge-transfer behavior. The energy-loss feature at around 4 eV exhibits predominant $4f^0$ character and shows the 4f hybridization strength can be attributed to charge transfer behavior. These results suggest different f-electron configurations for bulk and nanoparticle $CeAl_2$.

Fig. 3. Ce 4d-edge RIXS spectra of bulk (a) and nanoparticle (b) $CeAl_2$ recorded at selected excitation energies marked by the arrows d–f in the absorption spectrum. Spectra are displayed in energy-loss scale as the elastic peak is set at 0 eV.

References

[1] R.W. Keyes, Contemp. Phys. 32 (1991) 403.
[2] W. Halperin, Rev. Mod. Phys. 58 (1986) 533.
[3] Y.Y. Chen, T.D. Yao, T.K. Lee, C. Tse, W.C. Liu, H.C. Chang, K.T. Lin, Y.S. Lin, Z.C. Wang, W.H. Li, Chin. J. Phys. 36 (1998) 468.
[4] C.D. Bredl, F. Steglich, K.D. Schotte, Z. Phys. B 29 (1978) 327.
[5] Y.Y. Chen, et al., Chin. J. Phys. 36 (1998) 468.
[6] B.T. Thole, G. van der Laan, J.C. Fuggle, G.A. Sawatzky, R.C. Karnatak, J.-M. Esteva, Phys. Rev. B 32 (1985) 5107.
[7] J.C. Fuggle, F.U. Hillebrecht, J.-M. Esteva, R.C. Karnatak, O. Gunnarsson, K. Schönhammer, Phys. Rev. B 27 (1983) 4637.
[8] K. Starke, et al., Phys. Rev. B 55 (1997) 2672.
[9] K. Ichikawa, A. Nisawa, K. Tsutsumi, Phys. Rev. B 34 (1986) 6690.
[10] S.R. Mishra, R.R. Cummins, G.D. Waddill, W.J. Gammon, G. van der Laan, K.W. Goodman, J.G. Tobin, Phys. Rev. Lett. 81 (1998) 1306.

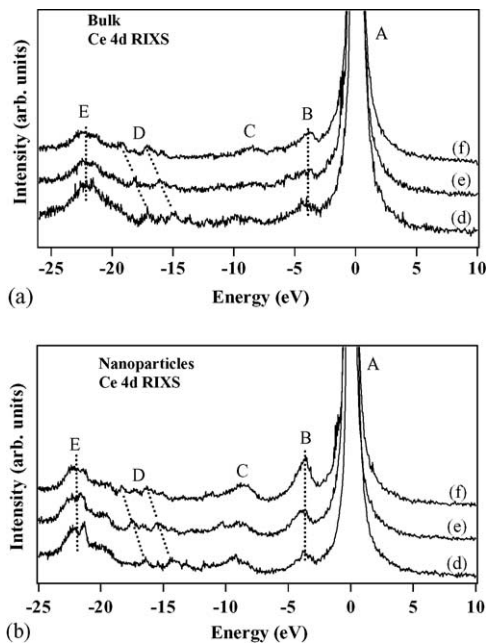[11] D. Wieliczka, J.H. Weaver, D.H. Lynch, C.G. Olson, Phys. Rev. B 26 (1982) 7056.

[12] C.L. Dong, C.L. Chen, C.L. Chang, Y.Y. Chen, in press.

[13] S.M. Butorin, L.-C. Duda, J.-H. Guo, N. Wassdahl, J. Nordgrent, M. Nakazawa, A. Kotani, J. Phys. Condens. Matter 9 (1997) 8155.

[14] J.-E. Rubensson, J. Lüning, S. Eisebitt, W. Eberhardt, Appl. Phys. A 65 (1997) 91.

[15] S.M. Butorin, M. Magnuson, K. Ivanov, D.K. Shuh, T. Takahashi, S. Kunii, J.-H. Guo, J. Nordgren, J. Electron Spectrosc. Relat. Phenom. 101–103 (1999) 783.

[16] A. Moewes, A.V. Postnikov, E.Z. Kurmaev, M.M. Grush, D.L. Ederer, Europhys. Lett. 49 (5) (2000) 665.

[17] D.R. Mueller, C.W. Clark, D.L. Ederer, J.J. Jia, W.L. O'Brien, Q.Y. Dong, T.A. Calcott, Phys. Rev. A 52 (1995) 4457.

[18] C.L. Dong, C.L. Chen, C.L. Chang, Y.Y. Chen, J.-H. Guo, in progress.

[19] A. Moewes, S. Stadler, R.P. Winarski, D.L. Ederer, M.M. Grush, T.A. Callcott, Phys. Rev. B 58 (1998) 15951.

[20] A. Moewes, D.L. Ederer, M.M. Grush, T.A. Callcott, Phys. Rev. B 59 (1999) 5452.